Numerical simulation of bi-stable ventilated flows around surface-piercing hydrofoils

Moran Charlou, Jeroen Wackers*
LHEEA, Ecole Centrale de Nantes/CNRS UMR 6298, Nantes/France
*jeroen.wackers@ec-nantes.fr

1 Introduction

Ventilation is a physical phenomenon in which air is entrained in a low pressure region below the free surface on a hydrofoil or a propeller. It is known to cause substantial drops of performance – lift for a hydrofoil or thrust for a propeller. Ventilation can be used to good advantage, like for drag reduction, but is most often unwanted.

On a surface-piercing lifting hydrofoil at high enough Froude numbers, two flow regimes exist: wetted when water completely covers both sides of the foil, and ventilated when a pocket of air covers a major part of the suction side. A wetted flow usually provides the best lift, whereas ventilation raises the pressure on the suction side and thus lowers the lift. The flow is in general wetted for low angles of attack and ventilated at high angles. However there is a range of angles in between, where both flow regimes exist and are stable. In this bi-stable region, a perturbation can brutally change the flow regime from wetted to ventilated and conversely. Harwood et al. (2014, 2016), in accordance with previous research, identified two conditions on the wetted flow which are required for the existence of a ventilated flow:

- A zone of low pressure, i.e. pressure lower than the atmospheric pressure, so a pressure gradient can entrain air towards the suction side,
- A separated flow on the suction side, i.e. a recirculation bubble.

These two conditions are necessary for stable ventilation, but not sufficient for the spontaneous transition to ventilated flow, since this requires the air to break through the attached flow with atmospheric pressure at the free surface. This explains why both flows can be stable under the same conditions. Fig. 1 shows an example for a vertical hydrofoil at an angle of attack (yaw) of 12.5°. The wetted flow validates the conditions above and the ventilated flow shows a 33% drop in lift compared to the wetted flow.

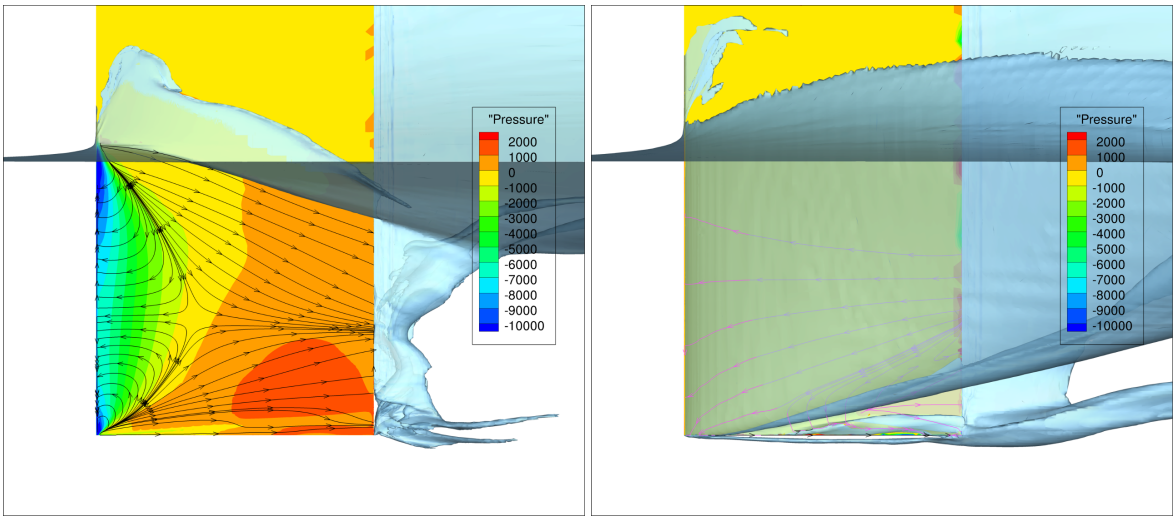

(a) Wetted (b) Ventilated

Fig. 1: Two flow regimes are stable at $\alpha = 12.5°$ and $Fn_h = 2.5$ (pressure, wall streamlines and free surface in a side view of the suction side).

Assessing the risk of ventilation in a bi-stable region through numerical simulation requires first, that the simulation should accurately represent the spontaneous or forced transition from wetted to ventilated flow. And second, when ventilation occurs it must remain stable even in the lower part of the bi-stable range for the angle of attack. The goal of this paper is to investigate these two conditions.

2 Test case

The test case is a vertical surface-piercing hydrofoil as studied in Harwood et al. (2014, 2016), and the present study varies the angle of attack α for a fixed immersion-based Froude number $Fn_h = 2.5$. In the experiments, for α between 2.5° and 15°, wetted flow was established naturally but ventilated flow could be obtained through a perturbation by a blast of air at the leading edge. However the required intensity of such a perturbation is uncertain. The present study instead focuses on natural transition by increasing α in steps of 2.5° through the bi-stable region until spontaneous ventilation occurs, and then decreasing it until the flow re-attaches to the foil, thus moving along a hysteretic cycle (Fig. 2a). The experiments were conducted in a towing tank at fixed α for each run, while the carriage was accelerated from zero to the target Fn_h for that run. If a hysteretic cycle occured, it was therefore along Fn_h and not α.

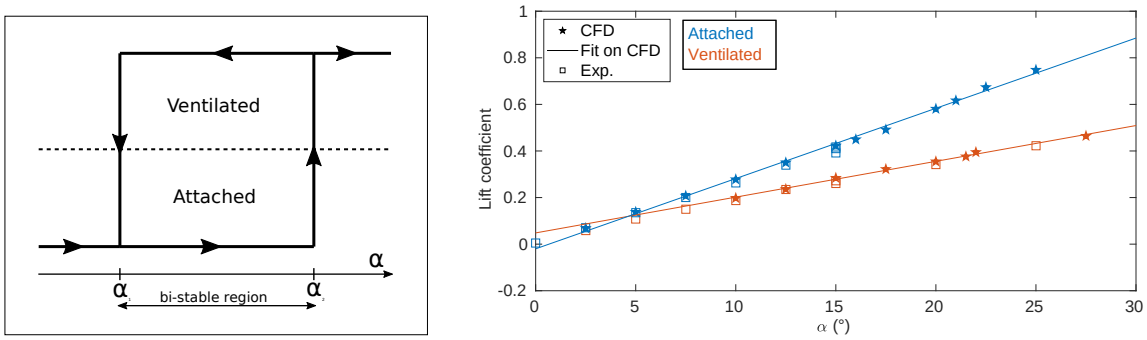

(a) Hysteretic cycle

(b) Lift coefficient: CFD *vs* Exp. from Harwood et al. (2016)

Fig. 2: Schematic representation of the hysteretic cycle and variation of the lift coefficient

The foil is symmetrical, has a chord $c = 0.279m$ with an ogival fore-body, a rectangular aft-body and a blunt trailing edge. The immersion depth is $h = c$. The computational domain is $6.7m$ wide with the foil centered, $4.05m$ high with $3.05m$ water depth and $9m$ long with the foil at 3m from the front.

The RANS solver used in this study is ISIS-CFD, a two-fluid solver developed by Ecole Centrale de Nantes/CNRS and part of NUMECA International's simulation suite FINE™/Marine. The water surface is represented with a water–air mixture surface capturing model using compressive discretisations, see Queutey and Visonneau (2007). Turbulence is solved with the $k-\omega\ SST$ (Menter) model. Adaptive grid refinement is used with a combined free-surface and pressure/velocity Hessian criterion, described in Wackers et al. (2017). The Hessian threshold is set at $0.05m$ ($\approx 0.18c$), the target cell size normal to the free surface is $c/100$ and the minimum cell size is $c/500$. The initial mesh is only refined around the foil. The flow is solved using a 1st-order accurate time-marching algorithm with a time step of $c/100U_\infty$, during which the refinement procedure is called every 20 steps. The size of the refined meshes goes from around 4M cells for a ventilated case to 9M cells for a wetted case.

Two methods were applied to start the computations: (a) increasing the speed of the foil from zero to reach the desired Fn_h, with α fixed, and (b) changing α at fixed speed (and Fn_h) from a previous computation. Method (a) was used to start computations from scratch, while method (b) was used to move along the hysteretic cycle in α.

Fig. 2b shows the lateral forces (lift) obtained in the hysteretic cycle, compared with the experimental data. These confirm that both the wetted and the ventilated states are predicted correctly. The transitions between the two flows are not indicated: these are discussed in the next sections.

3 Transition to a ventilated state

For the flow to transition from a wetted to a ventilated state, a path needs to open up between the surface and the recirculation bubble, through which air can flow. In the present case, the main air path runs down the leading edge to the low pressure peak in the bubble (Fig. 3). However, in the wetted state (Fig. 1a) this path is blocked by the attached flow at ambient pressure along the free surface. To obtain ventilation, this surface seal must be breached.

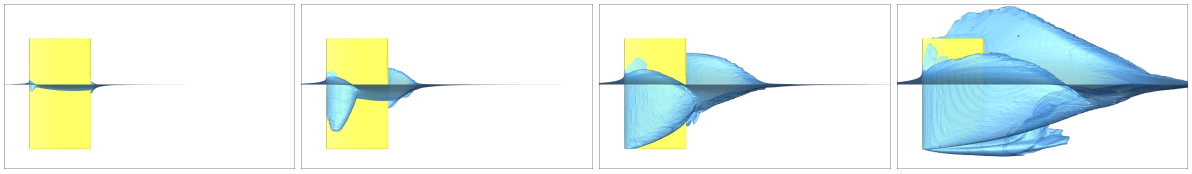

(a) $t \approx 0.10s$, $Fn_h \approx 1.2$ (b) $t \approx 0.17s$, $Fn_h \approx 1.9$ (c) $t \approx 0.24s$, $Fn_h \approx 2.4$ (d) $t \approx 0.37s$, $Fn_h = 2.5$

Fig. 3: Spontaneous ventilation inception at $\alpha = 21.5°$. The acceleration phase is 0.304s long.

In the experiments, spontaneous ventilation inception (above $\alpha = 15°$) is attributed to bubbles of air and turbulent vortex cores breaking the free surface at the leading edge. Such flows cannot be simulated with the present free-surface discretisation and RANS turbulence model, so the inception mechanism for the simulations is the full separation of the flow at the top of the leading edge (Fig. 3).

The simulations show that apart from the flow model, ventilation inception depends strongly on the path to the steady state. When increasing α at fixed $Fn_h = 2.5$ (method (b)), spontaneous ventilation occurs at 27.5°, when unsteady fluctuations of the wake start reaching the foil (Fig. 4). However, spontaneous ventilation occurs at angles as low as 12.5°, as opposed to 15° in the experiments, when accelerating slowly from zero speed like in Fig. 3 (method (a)). The reason for the difference between the two methods is that at Fn_h below 2.5, the wave behind the leading edge is shorter but steeper. This means that ventilation inception occurs more easily than at higher speeds. Thus, the inception takes place during the slow acceleration, after which the flow remains in the ventilated state until $Fn_h = 2.5$ is reached.

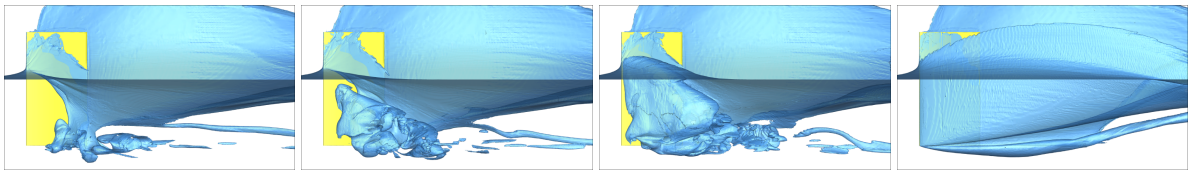

(a) $t \approx 0.24s$ (b) $t \approx 0.37s$ (c) $t \approx 0.44s$ (d) $t \approx 1.45s$

Fig. 4: Spontaneous ventilation inception when α increases from 25° to 27.5° at constant $Fn_h = 2.5$. The rotation phase is 0.202s long.

Thus, since ventilation transition depends more on *unsteady* – either transient or turbulent – phenomena than on the final steady flow conditions, we conclude that there is little practical interest in the investigation of spontaneous ventilation inception. Nature is rife with perturbations of all types, so the actual ventilation would never appear under the same circumstances as in simulation. It is more relevant to numerically evaluate the risk of ventilation occuring than to simulate actual transitions.

To assess the risk of ventilation in a given configuration, we recommend to simulate a big disturbance of the wetted flow, e.g. a sideways acceleration, sufficient to trigger at least a transient ventilated state. The stability of this ventilated flow after the disturbance has stopped determines if the configuration belongs to a bi-stable region. The stability of the wetted flow – i.e. how difficult it is to trigger ventilation – gives an insight into the likeliness of ventilation occuring in practice.

4 Stability of the ventilated state

Contrary to the inception, it is essential to simulate correctly the stability of the ventilated state, i.e. if it spontaneously returns to a wetted state or not. Otherwise, a bi-stable state may be incorrectly considered as free of ventilation risk. This requires the study of ventilation elimination.

In the experiments, elimination occurs when lowering Fn_h at fixed α. In that case, the ventilation pocket gradually closes from below, with a re-entrant jet on the foil surface rising steeper and steeper until it flows back to the leading edge and closes the ventilated pocket. However when lowering α at fixed Fn_h during simulations, ventilation elimination occurs at around 8°, as opposed to the 2.5° suggested by Harwood et al. (2016). With Fn_h staying at 2.5, the re-entrant jet remains on the lower side of the foil.

Instead of the ventilation pocket closing from below, the crest of water at the top of the pocket slowly hits the suction side and collapses, closing the air pocket and cutting off the air inflow. Without the inflow, the flow of air into the wake can no longer be sustained. Some air remains for some time in the recirculation zone, but ends up being chased out, leading to a wetted state (Fig. 5).

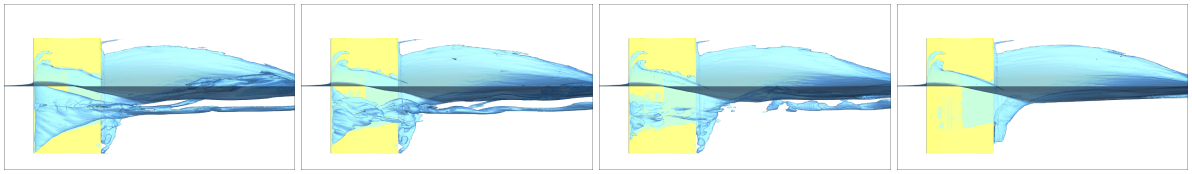

(a) $t \approx 1.51s$ (b) $t \approx 1.61s$ (c) $t \approx 1.71s$ (d) $t \approx 2.18s$

Fig. 5: Ventilation elimination at $\alpha = 7.5°$. $\alpha = 10°$ at $t = 0$, the rotation to 7.5° is done over 0.101s. A thin layer of air on the suction side is eliminated slowly because the speed is zero on the foil's surface.

To fully understand how the water crest collapses and closes the air pocket, the pressure and velocity in the air pocket are considered (Fig. 6). The top of the water crest over the pocket breaks and creates a bridge to the suction side of the foil. This zone of low water volume fraction prevents air from entering the pocket, further decreasing the naturally lower pressure in the air pocket, which in turn generates high velocities towards the inside of the pocket, pulling the water crest towards the foil. This vicious cycle ends up closing the air pocket from the top. Such a blocking effect might not occur if the breaking of the water crest was represented with drops of water instead of a diffuse low water fraction, making this specific issue inherent in the surface-capturing formulation used.

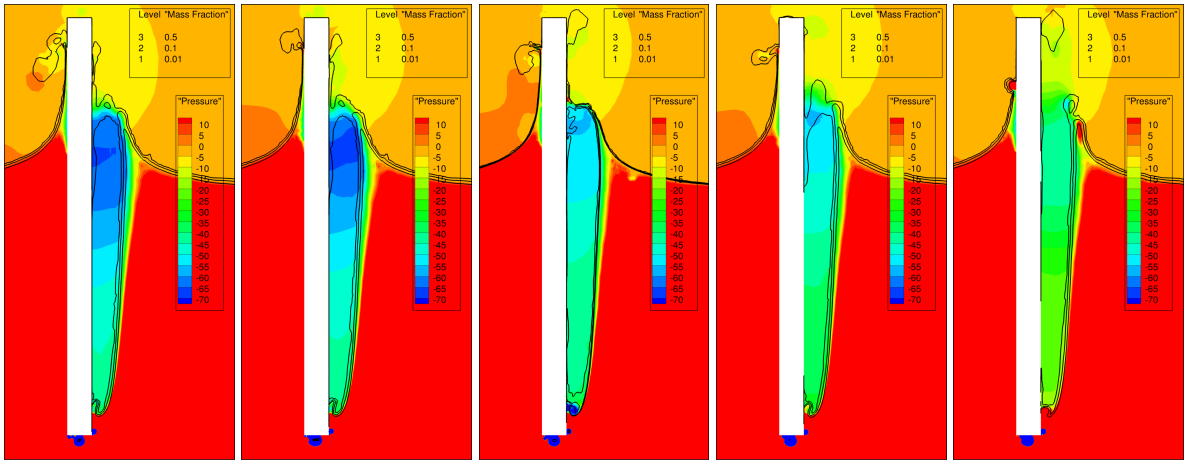

(a) Base parameters (b) Smaller time step, $\Delta t \approx$ 1.69e-4s (c) Refined free surface criterion (d) Surface tension $\sigma = 0.07N/m^{-1}$ (e) Surface tension $\sigma = 0.7N/m^{-1}$

Fig. 6: Slice of the ventilated pocket at $x = 0$ (mid-chord) for $\alpha = 10°$ and different numerical parameters. The pressure gradient introduced by the diffusion of low water fraction is responsible for the collapse of the air pocket.

Several attempt have been carried out to solve this problem. Because the compressiveness of the volume fraction scheme used in ISIS-CFD (Queutey and Visonneau (2007)) is sensitive to the local Courant number, the time step has been reduced. However as Fig. 6b shows, even though the local Courant number is divided by 4, that does not change the diffusion of the water fraction at the crest. Increasing the mesh refinement at the free surface in order to get a finer representation of the water-air interface reduces the induced pressure gradient – at the cost of computational speed – but does not remove the low volume fraction bridge (Fig. 6c). Finally, a surface tension model, based on Brackbill et al. (1992) but with the surface tension included in the pressure gradient, removed the bridge when using a surface tension 10 times higher than in reality (Fig. 6e). However, this changes some other features of the flow and intro-

duces additional numerical problems (e.g. unstable forces created by non-physical pressures on the foil). Using the actual air-water surface tension $\sigma = 0.07N.m{-}1$ (Fig. 6d) yields similar results to refining the free surface (Fig. 6c) in terms of the pressure gradient, while reducing the amount of water arriving on the foil surface significantly.

As a follow-up, the rotation from 10° to 7.5° was repeated with the actual air-water surface tension. While the flow without surface tension reattaches (Fig. 7a, see also Fig. 5), the surface tension model maintains a stable ventilated state (Fig. 7b). However, the rotation rate to 7.5° was reduced for this computation and it was later found out that a sufficiently slow rotation rate on its own is enough to prevent the flow from reattaching (Fig. 7c). But in this last computation a sheet of water is present on the foil, which is removed by the surface tension model. This may be an indication that the surface tension reduces the risk of reattachment.

Thus, while the motion history of the foil must once again be taken into account, the two tests indicate that the physical and numerical modelling of the water crest is a factor in the ventilation elimination. However, only the simulation with an artificially high surface tension (Fig. 6e) produces the straight crest which is observed in images from the experiments. Also, the irregular surface pressure in Fig. 7b is problematic. These are indications that the current surface tension model is ill adapted for the diffused low volume fractions that appear in the wave crest. A more detailed study of the surface tension and surface-capturing models for this flow is planned for future work.

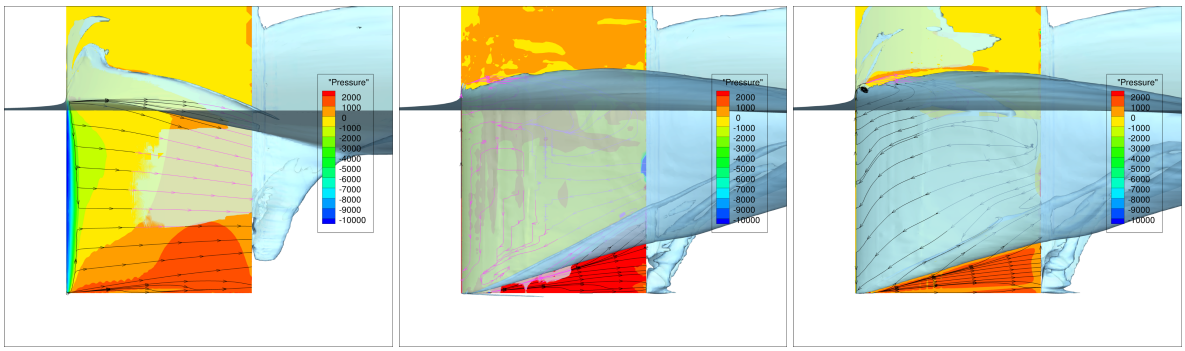

(a) Without surface tension, rotation over 0.101s

(b) With surface tension, rotation over 0.304s

(c) Without surface tension, rotation over 0.405s

Fig. 7: Both adding a surface tension model and slowing the rotation rate (coming from 10°) prevents the flow from rewetting at $\alpha = 7.5°$.

5 Conclusion

This paper studies the inception and stability of ventilation in bi-stable conditions. It is shown that spontaneous inception depends on the path to the steady state. Therefore, it is more relevant to provoke ventilation by artificial perturbation and to consider its stability, than to simulate spontaneous inception. At low angles of attack, the simulated ventilation is eliminated by a wave crest breaking and closing the ventilation pocket from the top. The tests show that this behaviour depends on the detailed physical and numerical modelling of the water sheet which forms the edge of the ventilating pocket.

Acknowledgements

This work was granted access to the HPC resources of the IDRIS computing centre under the allocation 2018/2019-A0052A01308 made by GENCI (Grand Equipement National de Calcul Intensif).

References

J.U. Brackbill, D.B. Kothe, and C. Zemach (1992). A continuum method for modeling surface tension. *J Comp Phys*, 100(2):335–354.

C.M. Harwood, Y.L. Young, and S.L. Ceccio (2016). Ventilated cavities on a surface-piercing hydrofoil at moderate Froude numbers: Cavity formation, elimination and stability. *J Fluid Mech*, 800:5–56.

C.M. Harwood, K.A. Brucker, F.M. Montero, Y.L. Young, and S.L. Ceccio (2014). Experimental and numerical investigation of ventilation inception and washout mechanisms of a surface-piercing hydrofoil. Proceedings of the 30th Symposium on Naval Hydrodynamics, Hobart, Australia.

P. Queutey and M. Visonneau (2007). An interface capturing method for free-surface hydrodynamic flows. *Comp Fluids*, 36(9):1481–1510.

J. Wackers, G. Deng, E. Guilmineau, A. Leroyer, P. Queutey, M. Visonneau, A. Palmieri, and A. Liverani (2017). Can adaptive grid refinement produce grid-independent solutions for incompressible flows? *J Comp Phys*, 334:364–380